Int. J. Heat Mass Transfer. Vol. 17, pp. 1–9. Pergamon Press 1974. Printed in Great Britain

AN ANALYSIS OF THE CONDUCTIVE AND RADIATIVE HEAT TRANSFER TO THE WALLS OF FLUIDIZED BED COMBUSTORS

V. N. VEDAMURTHY and V. M. K. SASTRI
Department of Mechanical Engineering, Indian Institute of Technology, Madras 600036, India

(*Received* 22 *September* 1972 *and in revised form* 11 *May* 1973)

Abstract—The conductive and radiative heat transfer to the walls of a Fluidized Bed Combustor are calculated. As a simplified model, the coal and ash particles are assumed to be spherical and the bed is considered to be vigorously bubbling. The analysis is one dimensional and is based on a gas film–emulsion packet model. The problem is formulated in terms of a non-linear partial differential equation assuming the gas film to be radiatively transparent and the emulsion packet to radiate as layers of black bodies. The solution is obtained numerically by the Crank–Nicolson method. The conductive and radiative specific heat fluxes and heat transfer coefficients for the emulsion and bubble phases are calculated at different fluidizing velocities, bed temperatures and particle sizes. The analytical results are shown to be in good agreement with the results reported in literature.

NOMENCLATURE

T, temperature of the emulsion [°K];
T_w, temperature of the wall surface [°K];
T_b, temperature of the core of the bed [°K];
t, time [h];
t_r, residence time of the emulsion packet at the surface of the gas film [h];
k, thermal conductivity [W/m² h °C];
C_p, specific heat [J/kg °C];
ρ, density [kg/m³];
σ, Stefan–Boltzman's const.;
U_{mf}, minimum fluidizing velocity [m/h];
U, fluidizing velocity [m/h];
d_p, average dia of the bed particles [m];
ε_{mf}, void ratio of the bed at minimum fluidization;
ε_f, void ratio of the bed at fluidizing velocity U;
H_{mf}, height of the bed at minimum fluidization [m];
H_f, height of the bed at fluidizing velocity U [m];
ΔX, finite difference between emulsion layers used in the numerical solution;
$\Delta\tau$, Time increment between two iterative steps in the numerical solution;
q_t, overall specific heat flux [kW/m²];
q_c, conductive specific heat flux [kW/m²];
q_r, radiative specific heat flux [kW/m²];
q_e, specific heat flux through emulsion phase [kW/m²];
q_b, specific heat flux through bubble phase;
F, view factor for radiant interchange (assumed to be unity);
Re_{mf}, Reynolds number corresponding to minimum fluidizing velocity;
Pr, Prandtl number of air at bed temperature;
k'_e, thermal conductivity coefficient of emulsion [5];
f_0, fraction of area covered by bubbles;
G_{mf}, mass velocity corresponding to U_{mf};
G_f, mass velocity corresponding to U;
μ, viscosity of fluidizing gas [kg/hm²].

Subscripts

s, solid;
g, gas;
e, emulsion;
m, node m;
$m-1$, node $m-1$;
$m+1$, node $m+1$;
M, last node;
0, surface node.

Superscripts

(v), time interval v;
$(v+1)$, time interval $v+1$.

INTRODUCTION

THE SUCCESSFUL adaptation of the fluidization technique in a wide range of process industries involving endothermic and exothermic reactions has, of late, given rise to extensive research on the development of fluidized bed combustors for use in industrial and power boilers. The factor of paramount importance behind this development is the high rate of bed-wall and bed-tube heat transfer.

McLaren and Williams [1], using coal of size −1·6 mm (10 B.S.S. Mesh), fluidizing velocities of 0·3–1·2 m/s and bed temperature of 700°C to 800°C have reported average bed-tube heat transfer coefficients of 530 W/m^2 °C for straight tubes and 465 W/m^2 °C for looped tubes. Vakrushev *et al.* [2] have reported bed-tube coefficients ranging from about 320 W/m^2 °C to 520 W/m^2 °C for a bed of hot coke of less than 1·0 mm dia, at temperatures of 200–650°C and fluidizing velocities of 0·2–0·75 m/s. Wright *et al.* [3] have reported average heat transfer rates of 180 kW/m^2 to various arrangements of tubes immersed within a fluidized bed with particle size ranging from 3·2 mm and 6·4 mm to 0·5 mm and operating between 850°C and 900°C at a fluidizing velocity of about 4 m/s. They also estimate that radiation contributes between 30 and 50 per cent of the heat transfer. But, Karchenko and Makhorin [4], while investigating the heat transfer between a copper-alpha calorimeter and a fluidized bed using narrow size fractions of quartz sand (about 0·34 mm mean dia) and fire clay (0·34–1·66 mm) over bed temperatures up to 1050°C have observed a linear relationship between the total heat transfer coefficient and bed temperature and contend that this is due to the changes in physical properties of the fluidizing gas and hence there is no appreciable amount of radiant heat transfer. Gelperin and Einstein [5] also support the view that at temperatures below 1000°C, the radiative component is usually small (not more than 5 per cent).

Considering the fact that heat transfer coefficient decreases with increase in particle diameter, it can be stated that there is general agreement about the value of the heat transfer coefficients at high temperatures but there is a wide difference of opinion about the quantitative contribution of radiation.

It is, thus, the aim of this paper to estimate the bed-wall conductive and radiative heat transfer at temperatures likely to be encountered in fluidized bed combustors.

MECHANISM OF HEAT TRANSFER

As the bed is assumed to be vigorously bubbling, the wall surface will be wetted not only by the continuous phase but also by the bubble phase and heat will flow from the core of the bed to the wall surface through these two phases. The heat transfer from the core of the bed to the wall surface through the bubble phase will be predominantly by radiation and that through the continuous phase by both conduction and radiation.

To analyse the mechanism of heat transfer through the continuous phase, a number of models have been proposed. Wicke and Fetting [6] proposed a twin layer model consisting of a gas film adjoining the bed wall surface and a solids boundary layer separating this film from the core of the bed. The heat flow through the gas layer was considered to be by conduction. But Mickley and Fairbanks [7] postulated that heat is transferred between the wall and the bed by emulsion packets of the solid and gaseous elements which, emanating from the core of the bed, reside at the wall surface for a short while, to be swept away and replaced by a fresh emulsion packet.

As the coal and ash particles in a fluidized bed combustor will be surrounded by a cloud of air and products of combustion, it will be more appropriate to consider the 'solids boundary layer' as proposed by Wicke and Fetting to be consisting of the emulsion packets proposed by Mickley and Fairbanks. Hence, in the present analysis, it will be assumed that during heat transfer through the continuous phase, the thermal barrier between the core of the bed and the wall surface consists of a gas film and an emulsion packet in contact with it as shown in Fig. 1. This

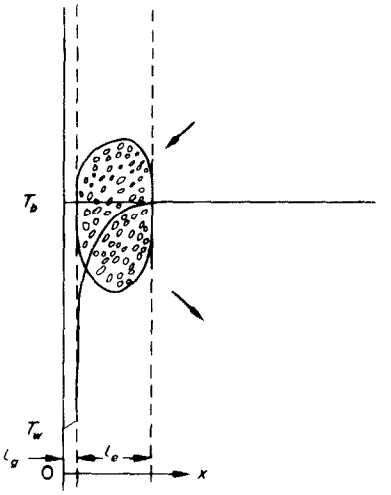

FIG. 1. The physical model.

packet is assumed to emanate from the core of the bed, reside at the gas film for a short while, and then, on being replaced by a fresh packet or a bubble rejoin the core. The gas film is assumed to be 0·5 d_p thick with thermal conductivity equal to that of the emulsion [5] and radiatively transparent. The emulsion packet is assumed to be $3d_p$ thick [10] and consists of layers of solid and gaseous elements which radiate as black bodies. The coal particles are

further assumed to be spherical and the bed considered to behave as a vigorously bubbling one with the wall surface exchanging radiation as a black body.

MATHEMATICAL FORMULATION AND SOLUTION

Heat will flow from the emulsion packet in contact with the gas film to the wall surface by (i) conduction through the gas film and (ii) radiative interchange of heat between the emulsion packet and the wall surface during the period of contact.

For a one-dimensional system, the governing energy equation for the emulsion layer in contact with the gas film can be written as

$$\rho_e C_{pe} \frac{\partial T}{\partial t} = ke \frac{\partial^2 T}{\partial x^2} + \frac{\partial}{\partial x}(q_r)$$

where

$$q_r = \sigma F_e (T^4 - T_w^4). \tag{1}$$

As the wall temperature is constant, equation (1) can be simplified as

$$\frac{\partial T}{\partial t} = \alpha_e \frac{\partial^2 T}{\partial x^2} + \beta_e T^3 \frac{\partial T}{\partial x}$$

where

$$\alpha_e = \frac{k_e}{\rho_e C_{pe}} \text{ and } \beta_e = \frac{4\sigma F_e}{\rho_e C_{pe}}. \tag{2}$$

It may be quite reasonably assumed that q_r for the ith emulsion layer is given by $q_r = \sigma F_e (T_i^4 - T_{i-1}^4)$. However, since T_{i-1} is known from the marching solution, equation (2) can be applied for the emulsion packet in discrete layers subject to the following initial and boundary conditions:

$$\text{At } t = 0, \quad T = T_b \qquad x > l_g \tag{3a}$$

$$x = l_g + l_e, \quad T = T_b \qquad t \geqslant 0. \tag{3b}$$

The other boundary condition will be obtained by applying the energy equation at the gas film emulsion layer interface.

Dimensionless forms of equations (2)–(3) can be obtained by defining

$$\theta = \frac{T}{T_b}$$

$$\tau = \frac{t}{t_r}$$

and

$$X = \frac{x - l_g}{l_e}.$$

Hence equations (1)–(3) become

$$\frac{\partial \theta}{\partial \tau} = \alpha \left(\frac{\partial^2 \theta}{\partial X^2} \right) + \beta \theta^3 \left(\frac{\partial \theta}{\partial X} \right) \tag{4}$$

where

$$\alpha = \frac{\alpha_e t_r}{l_e^2} \text{ and } \beta = \frac{\beta_e T_b^3 t_r}{l_e}.$$

At

$$\tau = 0, \quad \theta = 1 \qquad X > 0 \tag{5}$$

$$X = 1, \quad \theta = 1 \qquad \tau \geqslant 0. \tag{6}$$

Equation (4) is a nonlinear partial differential equation and is solved by a finite difference method [8].

Dividing the emulsion layer into M segments, each of thickness ΔX, equation (4) can be written, for all interior nodes, as

$$\frac{\partial \theta_m}{\partial \tau} = \alpha \left[\frac{\theta_{m-1} - 2\theta_m + \theta_{m+1}}{(\Delta X)^2} \right] + \beta \theta_m^3 \left[\frac{\theta_{m+1} - \theta_{m-1}}{2\Delta X} \right]. \tag{7}$$

Using Crank–Nicolson's method,

$$\theta_m^{(v+1)} = \theta_m^{(v)} + \tfrac{1}{2} \left[\left. \frac{\partial \theta_m}{\partial \tau} \right|^{(v)} + \left. \frac{\partial \theta_m}{\partial \tau} \right|^{(v+1)} \right] \Delta\tau. \tag{8}$$

Substituting (7)

$$\theta_m^{(v+1)} = \theta_m^{(v)} + \tfrac{1}{2} \left\{ \alpha \left[\frac{\theta_{m-1} - 2\theta_m + \theta_{m+1}}{(\Delta X)^2} \right]^{(v)} + \beta \left[\theta_m^3 \frac{\theta_{m+1} - \theta_{m-1}}{2\Delta X} \right]^{(v)} + \alpha \left[\frac{\theta_{m-1} - 2\theta_m + \theta_{m+1}}{(\Delta X)^2} \right]^{(v+1)} + \beta \left[\theta_m^3 \frac{\theta_{m+1} - \theta_{m-1}}{2\Delta X} \right]^{(v+1)} \right\}. \tag{9a}$$

As a simplification it is assumed that $\theta_m^{(v)^3} = \theta_m^{(v+1)^3}$. Then equation (9a) reduces to

$$\theta_{m-1}^{(v+1)} [-p + q\theta_m^{(v)^3}] + \theta_m^{(v+1)} [2 + 2p] + \theta_{m+1}^{(v+1)} [-p - q\theta_m^{(v)^3}] = \theta_{m-1}^{(v)} [p - q\theta_m^{(v)^3}] + \theta_m^{(v)} [2 - 2p] + \theta_{m+1}^{(v)} [p + q\theta_m^{(v)^3}] \tag{9b}$$

where

$$p = \frac{\alpha \Delta\tau}{(\Delta X)^2} \text{ and } q = \frac{\beta \Delta\tau}{2\Delta X}.$$

Last node

It follows from the boundary condition, equation (6), that

$$\theta_{M+1} = 1. \tag{10}$$

Surface node

The conductive and radiative heat fluxes entering and leaving the surface node are shown in Fig. 2.

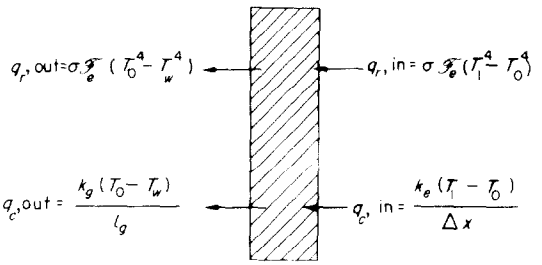

FIG. 2. The surface node.

Applying energy equation,

$$\rho_e C_{pe} \frac{\Delta X}{2} \frac{\partial T_0}{\partial t} = \left[\frac{k_e}{\Delta X}(T_1 - T_0) + \sigma F_e (T_1^4 - T_0^4)\right] - \left[\frac{k_g}{l_g}(T_0 - T_w) + \sigma F_e (T_0^4 - T_w^4)\right].$$

Non-dimensionalization and application of Crank–Nicolson's algorithm to this equation results in

$$\theta_0^{(v+1)}[2 + 2p + 2q\theta_0^{(v)3} + g] + \theta_1^{(v+1)}[-2p - q\theta_1^{(v)3}] = \theta_0^{(v)}[2 - 2p - 2q\theta_0^{(v)3} - g] + \theta_1^{(v)}[2p + q\theta_1^{(v)3}] + \theta_w[2g + 2q\theta_w^3] \quad (11)$$

where

$$g = \frac{2k_e t_r \Delta\tau}{\rho_e C_{pe} l_e l_g \Delta X}.$$

Equations (9)–(11) form a set of algebraic equations which, when solved, give the temperature at the time interval $(v + 1)$ in terms of its temperature at the time interval (v).

The instantaneous heat transfer to the wall surface through emulsion packets in contact with the gas film due to conduction through the gas layer and by direct radiant interchange between the emulsion packet and wall surface is given by

$$q_e = (q_c + q_{re})(1 - f_0)$$

where

$$q_c = \frac{k_g}{l_g}(T_0 - T_w)$$

and

$$q_{re} = \sigma F_e (T_0^4 - T_w^4).$$

The instantaneous heat transfer to the wall surface through bubbles in contact with the gas film by direct radiant interchange between the core of the bed and the wall surface, assuming the bubble phase as radiatively transparent, is given by

$$q_b = \sigma F (T_b^4 - T_w^4) f_0.$$

As an approximation, F_e and F are assumed as unity. Assuming a uniform residence time for the various emulsion packets, the temporal mean of the heat flux may be taken as the arithmetic mean of the instantaneous values.

In the present analysis, the above equations were solved on a digital computer with a step size of $\frac{1}{30}$ and time variation of $\frac{1}{20}$ of the average residence time. The bed height at minimum fluidization was assumed to be 250 mm. The analysis was carried out for fluidization velocities ranging from 1·25 to 8 times the value of that at minimum fluidization. The mean particle size was varied from 0·5 to 3 mm in steps of 0·5 mm and the bed temperature was varied from 800°C to 1100°C in steps of 100°C. The physical properties of the gas film and the gases in the core of the bed were assumed to be equal to those of air at corresponding bed temperatures.

The formulae used for determining the bed parameters and the physical properties of air and ash used in the computation are given in the Appendices.

RESULTS AND DISCUSSION

The variation of the temperature of the emulsion packet along its length at the end of the average residence time, i.e. when it is about to rejoin the core of the bed, is shown in Figs. 3(a) and 3(b). It can be seen that the temperature level increases with increase in fluidizing velocity. This may be explained by the decrease in average residence time of the packets at the gas film as the velocity increases. The temperature level also increases with increase in particle size. This is due to the increase in thickness of the gas film with increase in particle size which increases the thermal resistance for conductive heat transfer and reduces the cooling rate. It can also be seen that the cooling of the emulsion packet is limited only to a distance of about 1·5 d_p, thus proving the validity of the boundary condition 3(b). This is also in close agreement with the finding of A.I. Ilchenko *et al.* [12] who, while studying the degree of cooling of particles on individual water cooled tubes, have found that cooling extended only to a distance equal to d_p.

The variation of instantaneous specific heat flux with residence time of the emulsion packet at the surface of the gas film for a particle size of 0·5 mm and bed temperature of 900°C is shown in Figs. 4(a) and

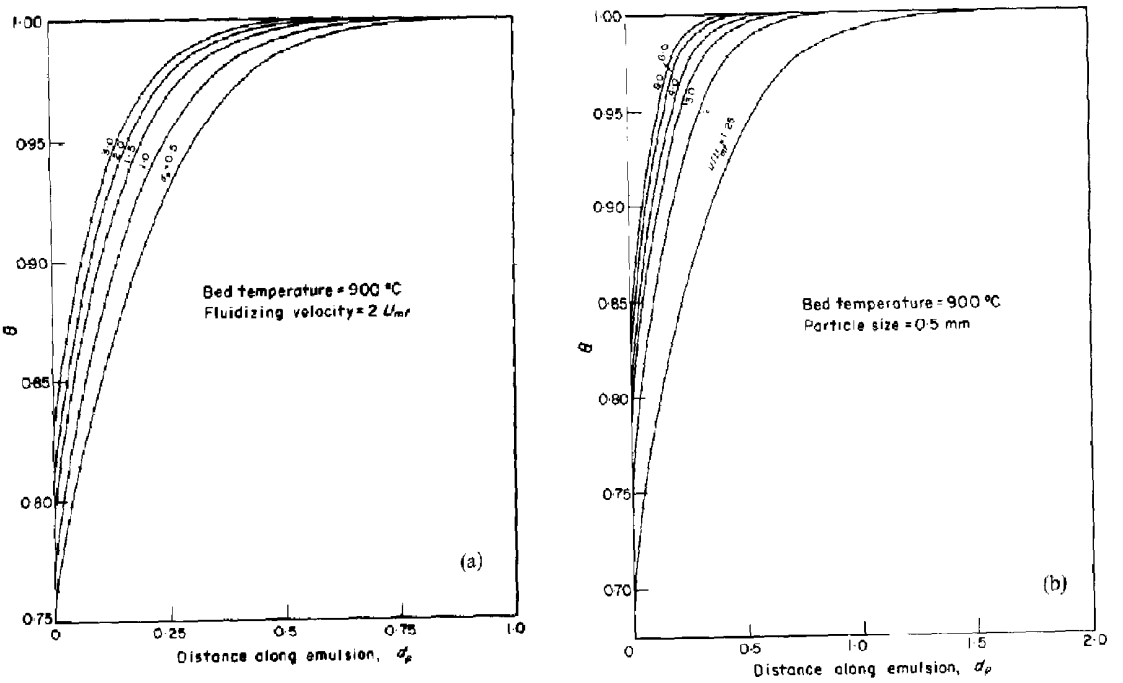

FIG. 3. (a) and (b). Variation of temperature along emulsion at the end of residence time.

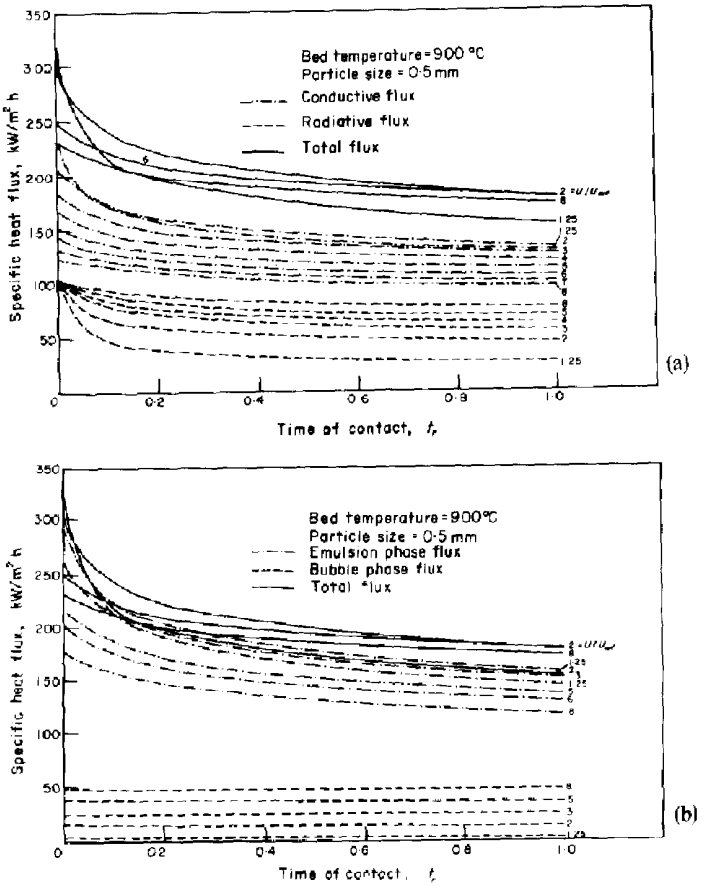

FIG. 4. (a) and (b). Variation of instantaneous heat flux with residence time.

4(b). It can be seen that radiation plays a significant role and contributes between 17 and 30 per cent of the total heat transfer. The instantaneous specific heat flux varies between 340 and 150 kW/m^2 h at 900°C. Considering the black body assumption, these values are in close agreement with the average value of 180 kW/m^2 h reported by Wright *et al.* [3]. However, their estimate of radiation contribution of 30–50 per cent of the total heat transfer at bed temperatures of 850 and 900°C appears to be somewhat on the high side. The radiative and bubble phase heat fluxes increase steadily with increase in fluidizing velocity, whereas the conductive flux has a maximum at twice the minimum fluidizing velocity. However, the total and emulsion phase heat fluxes initially increase with velocity and then decrease, the optimum values occurring at a velocity twice that for minimum fluidization.

The variation of the average overall heat transfer coefficient with fluidizing velocity is shown in Fig. 5(a). It increases initially with increase in velocity and then decreases after reaching a maximum. For a particle size of 0·5 mm, the maximum occurs at a velocity of about 2·5 times that for minimum fluidization. The same trend is observed for the conductive and emulsion phase coefficients also. However, the radiative and bubble phase coefficients do not exhibit such a trend and their values increase with velocity. This may be attributed to the increase in area of the gas film exposed to bubbles as velocity increases.

The variation of heat transfer coefficients with particle size at different fluidizing velocities is shown in Figs. 6(a) and 6(b). The conductive, emulsion phase and overall coefficients decrease with increase in particle size. The decrease is rapid initially but these

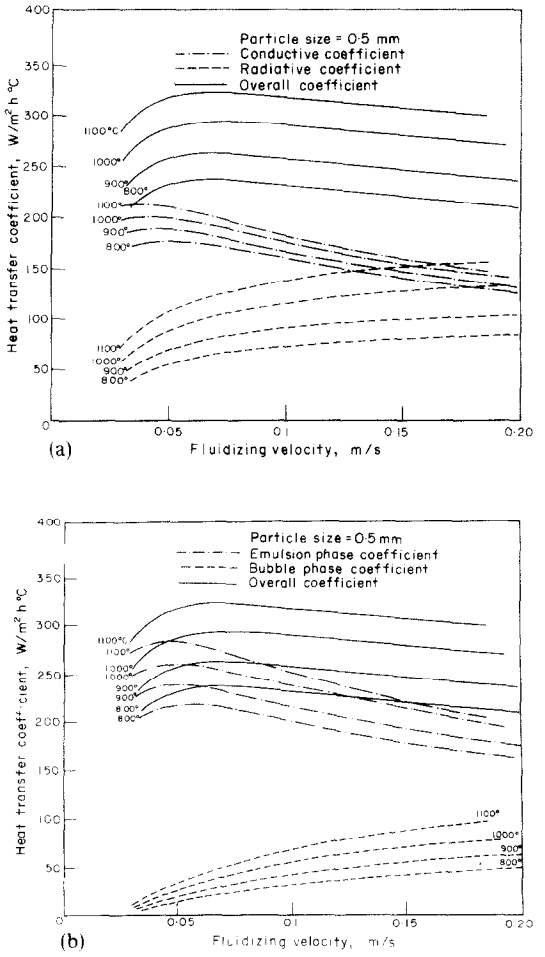

FIG. 5. (a) and (b). Variation of heat transfer coefficients with fluidizing velocity.

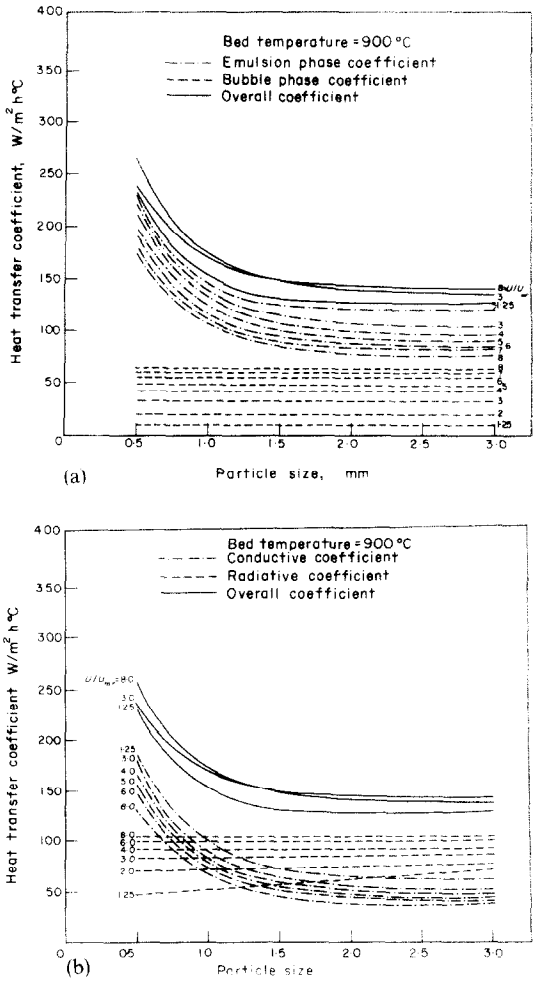

FIG. 6. (a) and (b). Variation of heat transfer coefficients with particle size.

values stabilize at particle sizes of 2·5–3 mm. The bubble phase coefficient is independent of particle size, but the radiative component increases with it and this could be due to higher temperature level of the emulsion packet which, in turn, is due to slower cooling caused by increased gas film thickness.

The variation of the heat transfer coefficients with bed temperature for various velocities for a particle size of 0·5 mm are shown in Fig. 7. It can be seen that

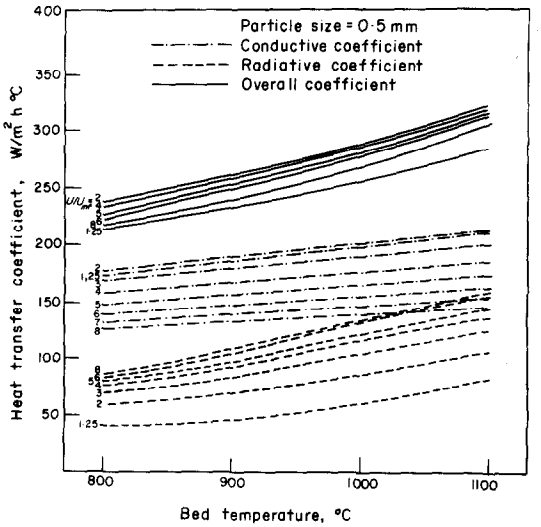

FIG. 7. Variation of heat transfer coefficients with bed temperature.

while the conductive component varies linearly with bed temperature, the other coefficients are nonlinear, especially as the temperature increases. However, Karchenko and Makhorin [4], while plotting the variation of experimentally observed maximum values of the overall heat transfer coefficients with bed temperatures have reported a linear relationship. A similar plot of the maximum value of the computed overall coefficients (Fig. 8) also shows a similar variation within a limit of 5 per cent. However, their claim that this is due to the linear variation of conductive heat transfer coefficient caused by the changes in physical properties of the gases and hence radiation is insignificant does not seem plausible. The present analysis, on the contrary, indicates that the variation of conductive and radiative components are both nonlinear but the nature of these variations is such that when the two components are added together, their nonlinearities seem to almost compensate each other resulting in a nearly linear variation of the maximum overall heat transfer coefficient with bed temperature.

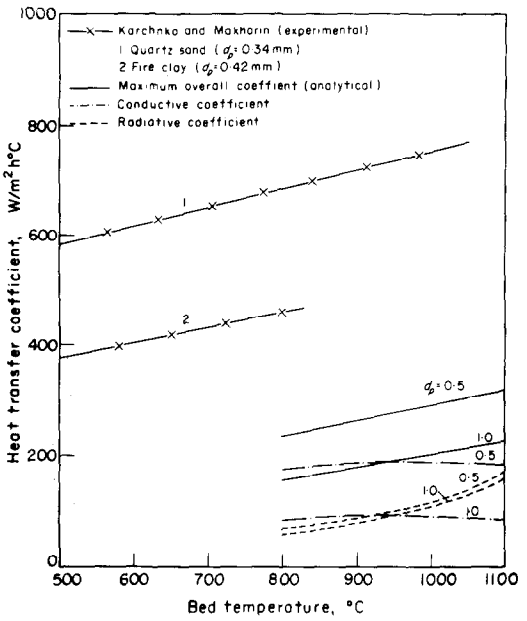

FIG. 8. Comparison of results.

CONCLUSION

The results obtained by the assumption of black body conditions at the wall surface and the emulsion overestimate the heat flux and heat transfer coefficients and this can be offset by suitably selecting the configuration factor. However, the nature of the variation of these values agree with the experimentally observed trends and hence this model can be used as a starting point in estimating the bed parameters. At the bed temperatures considered, the contribution of radiation is quite significant and cannot be neglected.

REFERENCES

1. J. McLaren and D. Williams. Combustion efficiency, sulphur retention and heat transfer in pilot plant fluidized bed combustors, *J. Inst. Fuel* **42**, 303–308 (1969).
2. I. A. Vakrushev, Ya. A. Botnikov and N. G. Zenchenkov, Heat transfer from a fluidized bed of hot coke to the surface of horizontal tubes, *Int. Chem. Engng* **3** (2), 207 (1963).
3. S. J. Wright, H. C. Ketley and R. G. Hickman, The combustion of coal in fluidized beds for firing shell boilers, *J. Inst. Fuel* **42**, 235–240 (1969).
4. N. V. Karchenko and K. E. Makhorin, The rate of heat transfer between a fluidized bed and an immersed body at high temperatures, *Int. Chem. Engng* **4** (4), 650–654 (1964).
5. N. I. Gelperin and V. G. Einstein, Heat Transfer in fluidized beds, *Fluidization*, Ch. 10, pp. 471–535. Academic (1971).

6. E. Wicke and F. Fetting, *Chem. Ing. Tech.* **26** (6), 301–309 (1954).
7. H. S. Mickley and D. F. Fairbanks, Mechanism of heat transfer to fluidized beds. *A.I.Ch.E. Jl* **1**, 374–384 (1955).
8. G. E. Myers, *Analytical Methods in Conduction Heat Transfer*. Ch. 8, pp. 233–314. McGraw-Hill (1971).
9. M. Mikheyev, *Fundamentals of Heat Transfer*, pp. 353–354. Peace Publishers, Moscow.
10. D. Kunii and O. Levenspiel, *Fluidization Engineering*, pp. 265–301. John Wiley (1969).
11. M. Leva *et al.*, Fluidization of solid nonvesicular particles. *Chem. Engng Prog.* **44** (8), 619–626 (1948).
12. A. I. Ilchenko, V. S. Pikashov and K. E. Makhorin, Study of radiative heat transfer in a fluidized bed, *J. Engng Phys.* **14** (4), 321–324 (1968).

APPENDIX I

Formulae Used in Determining Bed Parameters

$$U_{mf} = \frac{\mu}{d_p \rho_g}\left[(33{\cdot}7)^2 + 0{\cdot}0408\,\frac{d_p^3 \rho_g(\rho_s - \rho_g)g}{\mu^2}\right]^{\frac{1}{2}} - 33{\cdot}7 \qquad [10]$$

$$k_e = k_g\left[\frac{k'_e}{k_g} + 0{\cdot}15\,Re_{mf}Pr\right] \qquad [5]$$

$$t_r = \frac{H_{mf}}{0{\cdot}711\,H_f}\,\frac{(U - U_{mf})}{1{\cdot}5g}\left(\frac{H_{mf}}{H_f - H_{mf}}\right)^2 \qquad [5]$$

$$f_0 = 1 - \frac{H_{mf}}{H_f} \qquad [5]$$

$$H_f = H_{mf}\,\frac{(1 - \varepsilon_{mf})}{(1 - \varepsilon_f)} \qquad [10]$$

$$\frac{1 - \varepsilon_f}{\varepsilon_f^3} = \frac{G_{mf}}{G_f}\left(\frac{1 - \varepsilon_{mf}}{\varepsilon_{mf}^3}\right). \qquad [11]$$

APPENDIX II

Physical Properties of Air [9]

Temp (°C)	ρ (kg/m^3)	C_p (kcal/kg°C)	k_g (kcal/mh°C)	$U \times 10^6$ (kgs/m^2)	Pr
800	0·329	0·276	0·0617	4·52	0·713
900	0·301	0·280	0·0656	4·76	0·717
1000	0·277	0·283	0·0694	5·00	0·719
1100	0·257	0·286	0·0731	5·22	0·722

APPENDIX III

Physical Properties of Ash

Density—800 kg/m^3
Thermal conductivity—0·061 kcal/mh°C
Specific heat = 0·20 kcal/kg°C

ANALYSE DU TRANSFERT THERMIQUE AUX PAROIS PAR CONDUCTION ET RAYONNEMENT DANS DES CHAMBRES DE COMBUSTION A LIT FLUIDISE

Résumé—On calcule le transfert thermique par conduction et rayonnement aux parois d'une chambre de combustion à lit fluidisé. Dans un modèle simple, les particules de charbon et de cendre sont supposées être sphériques et le lit est supposé vigoureusement brassé. L'analyse est à une seule dimension et elle est basée sur un modèle film gazeux–émulsion en globules. Le problème conduit à une équation non linéaire aux dérivées partielles qui suppose que le film gazeux est transparent et que le paquet en émulsion rayonne comme des couches de corps noirs. La solution numérique est obtenue par la méthode de Crank–Nicolson. Les flux thermiques et les coefficients de transfert sont calculés pour différentes vitesses de fluidisation, pour plusieurs températures du lit et tailles de particules. Les résultats théoriques sont en bon accord avec les valeurs données dans la bibliographie.

EINE ANALYSE DER WÄRMELEITUNG UND WÄRMESTRAHLUNG FÜR WÄNDE VON WIRBELBETTBRENNERN

Zusammenfassung—Die Wärmeleitung und Wärmestrahlung der Wände von Wirbelbettbrennern wird berechnet. Als vereinfachtes Modell werden die Kohle und Aschepartikel als kugelförmig angenommen und das Bett wird als kräftig brodelnd betrachtet. Die Analyse ist eindimensional und basiert auf dem Modell einer gasförmigen Filmemulsionspackung. Das Problem wird unter den Bedingungen einer nichtlinearen partiellen Differentialgleichung formuliert, wobei angenommen wird, dass der Gasfilm strahlungsdurchlässig ist und die Emulsionspackung als Schichtung schwarzer Körper strahlt. Die Lösung wird numerisch mit Hilfe der Crank–Nicolson Methode gefunden.

Die konduktiven und strahlenden spezifischen Wärmeströme und Wärmeübergangskoeffizienten für die Emulsion und Blasenzustände werden bei verschiedenen Fliessgeschwindigkeiten, Bettemperaturen und Teilchengrössen berechnet. Es wird gezeigt, dass sich die analytischer Ergebnisse in guter Übereinstimmung mit den in der Literatur aufgeführten befinden.

ИССЛЕДОВАНИЕ КОНДУКТИВНОГО И ЛУЧИСТОГО ПЕРЕНОСА ТЕПЛА К СТЕНКАМ КАМЕР СГОРАНИЯ С ПСЕВДООЖИЖЕННЫМ СЛОЕМ

Аннотация—Дается расчет кондуктивного и лучистого переноса тепла к стенкам камеры сгорания с псевдоожиженным слоем. В принятой упрощенной модели предполагается, что частицы угля и золы являются сферическими, и в слое происходит интенсивное кипение. Анализ является одномерным и основывается на модели газовая пленка-эмульсионный пакет. Задача формулируется в виде нелинейного дифференциального уравнения в частных производных в предположении, что газовая пленка прозрачна для излучения, а эмульсионный пакет излучает тепло как абсолютно черное тело. Численное решение полгчено методом Кранка-Никольсона. Кондуктивные и лучистые удельные потоки тепла и коэффициенты теплообмена для эмульсионной и пузырьковой фаз рассчитываются при различных скоростях псевдоожижения, температурах слоев и размерах частиц. Показано, что аналитические результаты находятся в хорошем соответствии с опубликованными данными.